Supporting Information

for

Aliphatic C–C Bond Cleavage of α-Hydroxy Ketones by Nonheme Iron(II) Complexes: Mechanistic Insight into the Reaction Catalyzed by 2,4′-Dihydroxyacetophenone Dioxygenase

*Rubina Rahaman, Sayantan Paria, and Tapan Kanti Paine**

Department of Inorganic Chemistry, Indian Association for the Cultivation of Science,

2A & 2B Raja S. C. Mullick Road, Jadavpur, Kolkata 700032, India

Email: ictkp@iacs.res.in

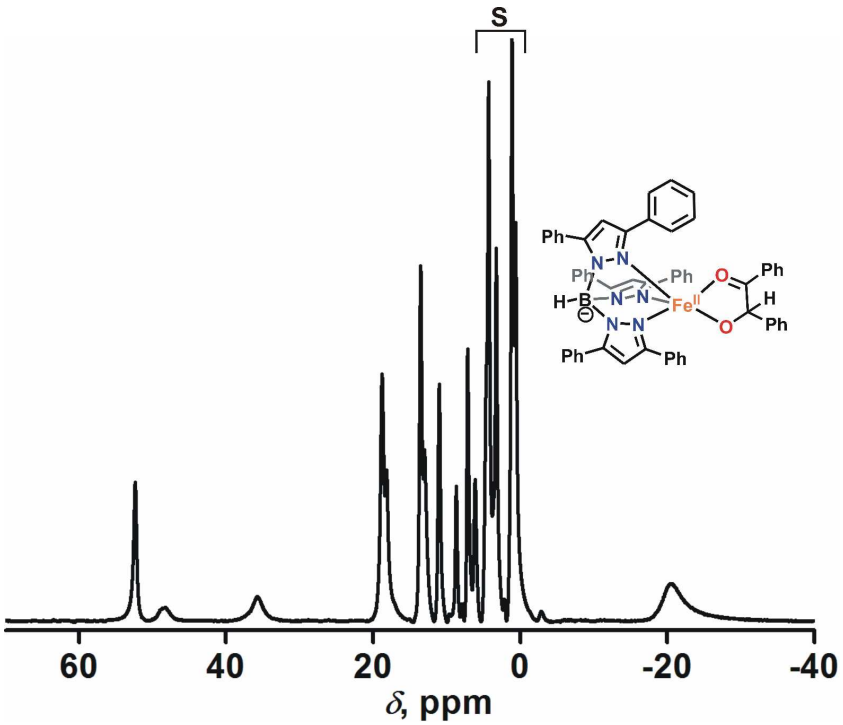

Figure S1 ^{1}H NMR (500 MHz, C_6D_6, 295 K) spectrum of [(Tp^{Ph2})Fe^{II}(PHAP)] (**1**). Peaks marked with 'S' are from residual solvents.

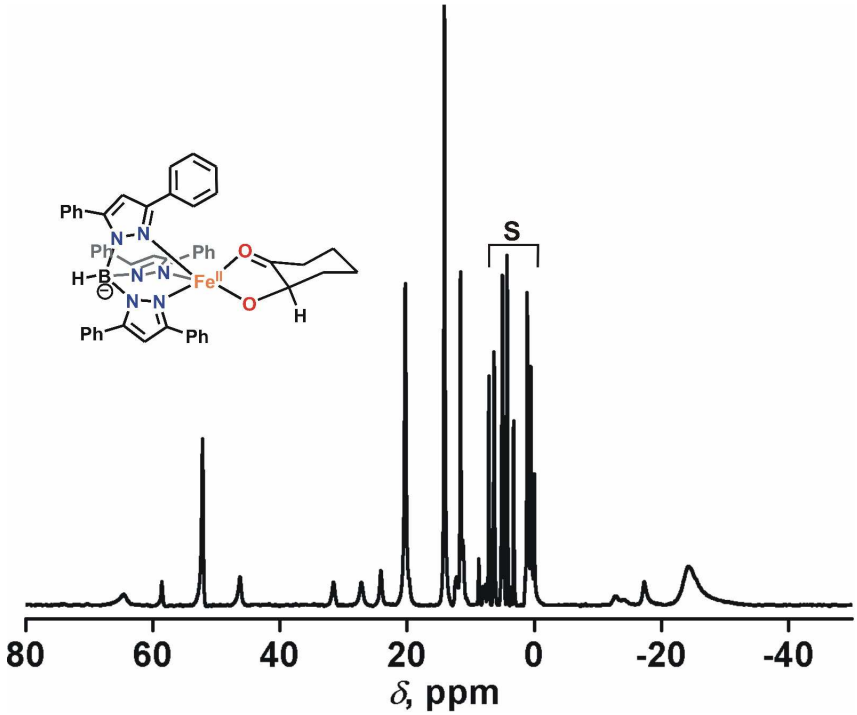

Figure S2 ^{1}H NMR (500 MHz, C_6D_6, 295 K) spectrum of [(Tp^{Ph2})Fe^{II}(HCH)] (**2**). Peaks marked with 'S' are from residual solvents.

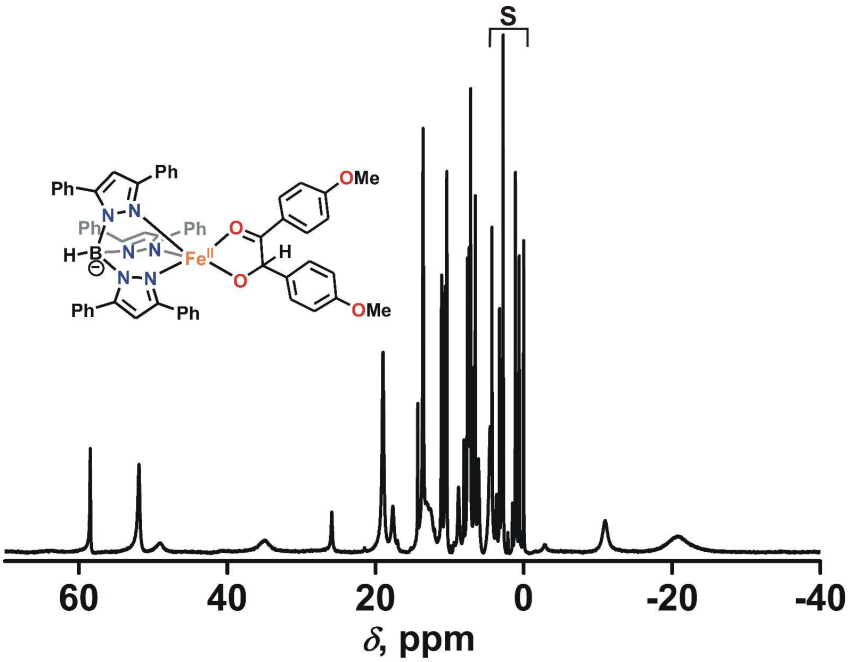

Figure S3 ^{1}H NMR (500 MHz, C_6D_6, 295 K) spectrum of [(Tp^{Ph2})Fe^{II}(HBME)] (**3**). Peaks marked with 'S' are from residual solvents.

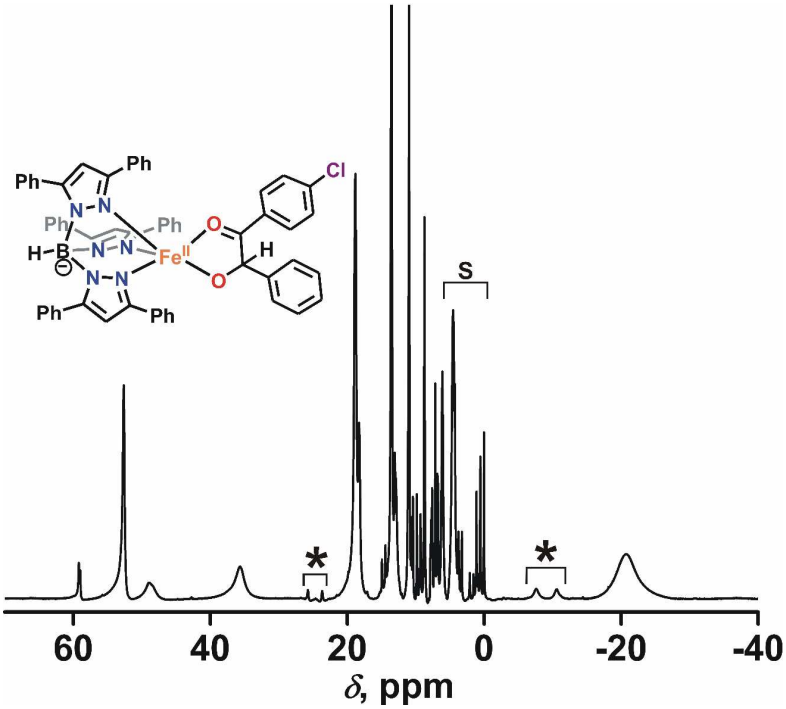

Figure S4 ^{1}H NMR (500 MHz, C_6D_6, 295 K) spectrum of [(Tp^{Ph2})Fe^{II}(CHPE)] (**4**). Peaks marked with 'S' are from residual solvents. *-Marked peaks arise from species formed upon partial oxidation of the complex.

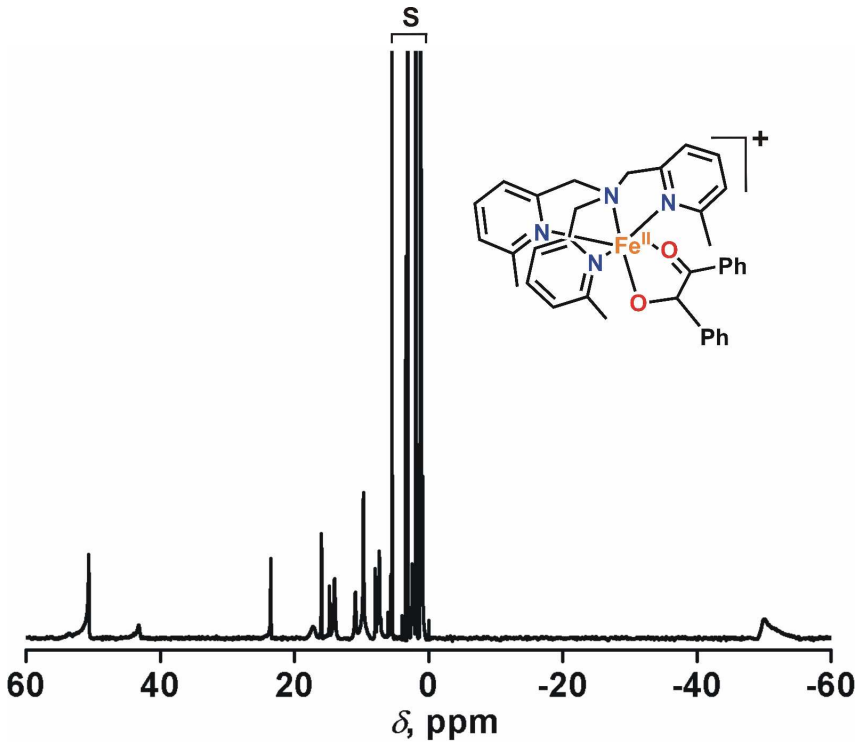

Figure S5 ^{1}H NMR (300 MHz, CD_3CN, 295 K) spectrum of [(6-Me_3-TPA)Fe^{II}(PHAP)](ClO_4) (**5**). Peaks marked with 'S' are from residual solvents.

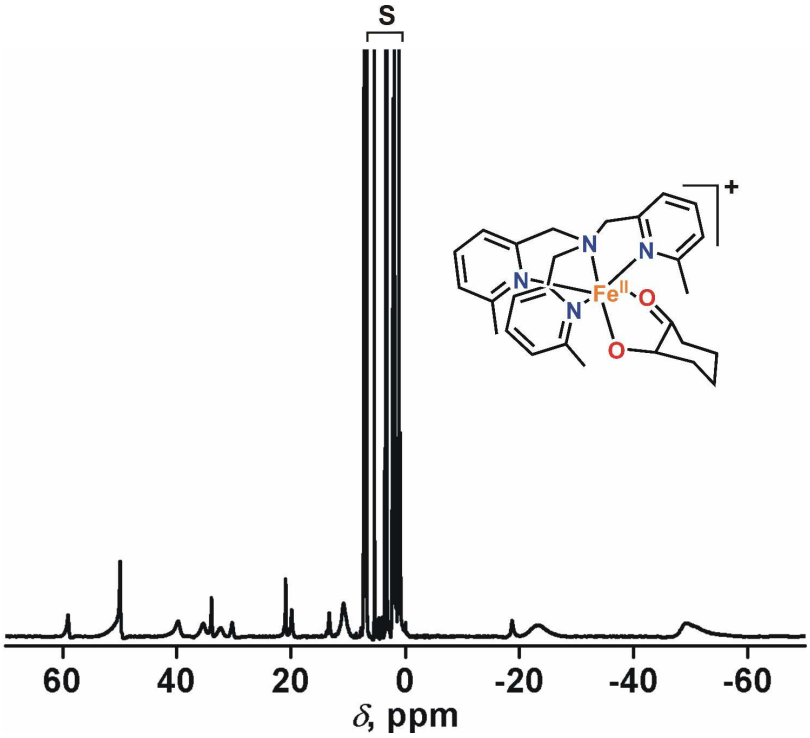

Figure S6 ^{1}H NMR (500 MHz, CD_3CN, 295 K) spectrum of [(6-Me_3-TPA)Fe^{II}(HCH)](BPh_4) (**6**). Peaks marked with 'S' are from residual solvents.

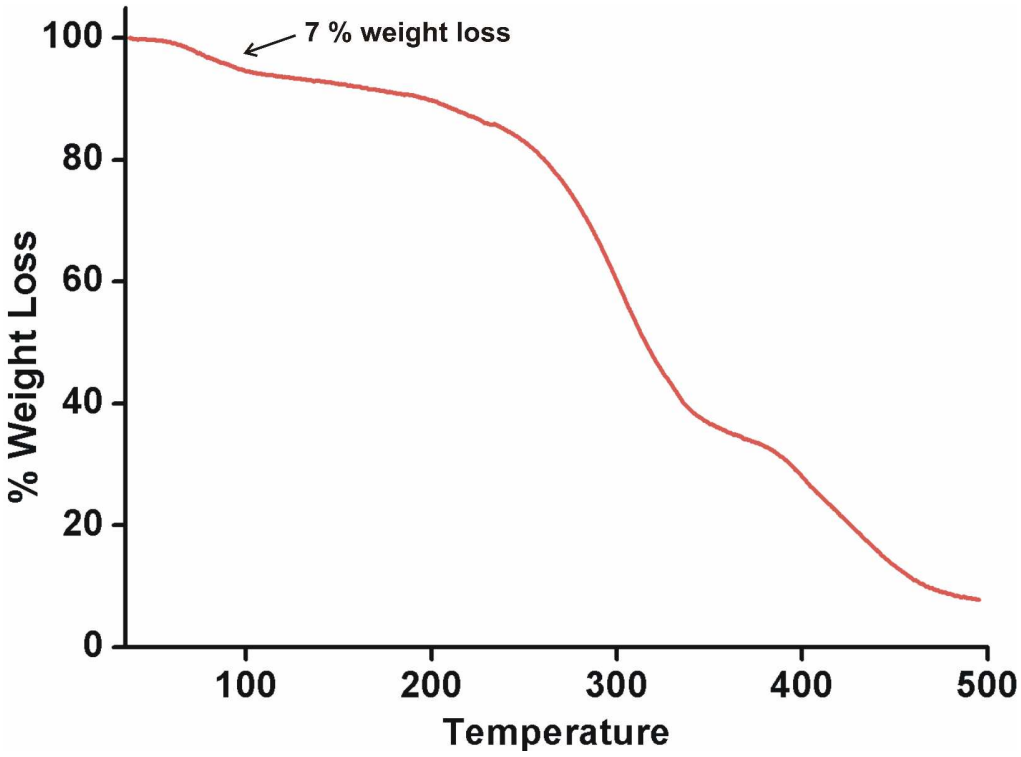

Figure S7 TGA curve for **1**·CH_2Cl_2.

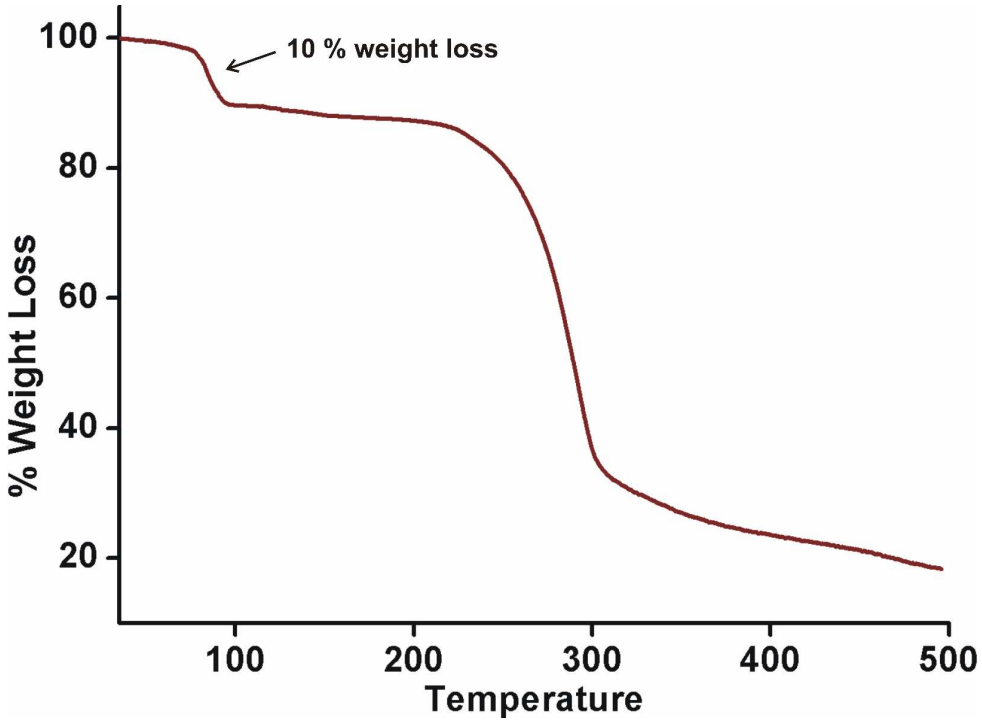

Figure S8 TGA curve for **2**·2CH_3OH.

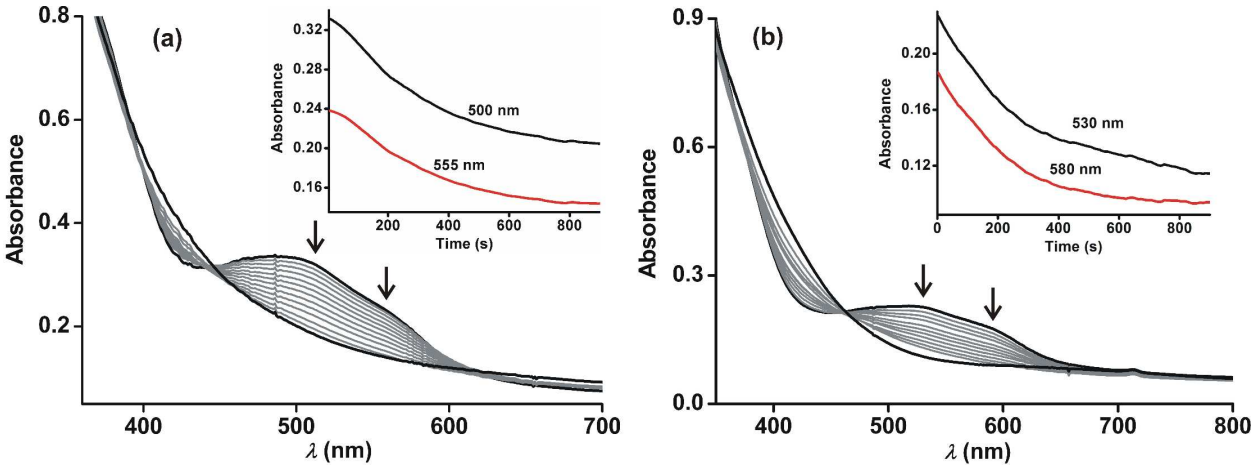

Figure S9 Optical spectral changes of (a) **3** and (b) **4** (0.5 mM in benzene) with time during the reaction with dioxygen at 283 K. Insets: absorbance as a function of time.

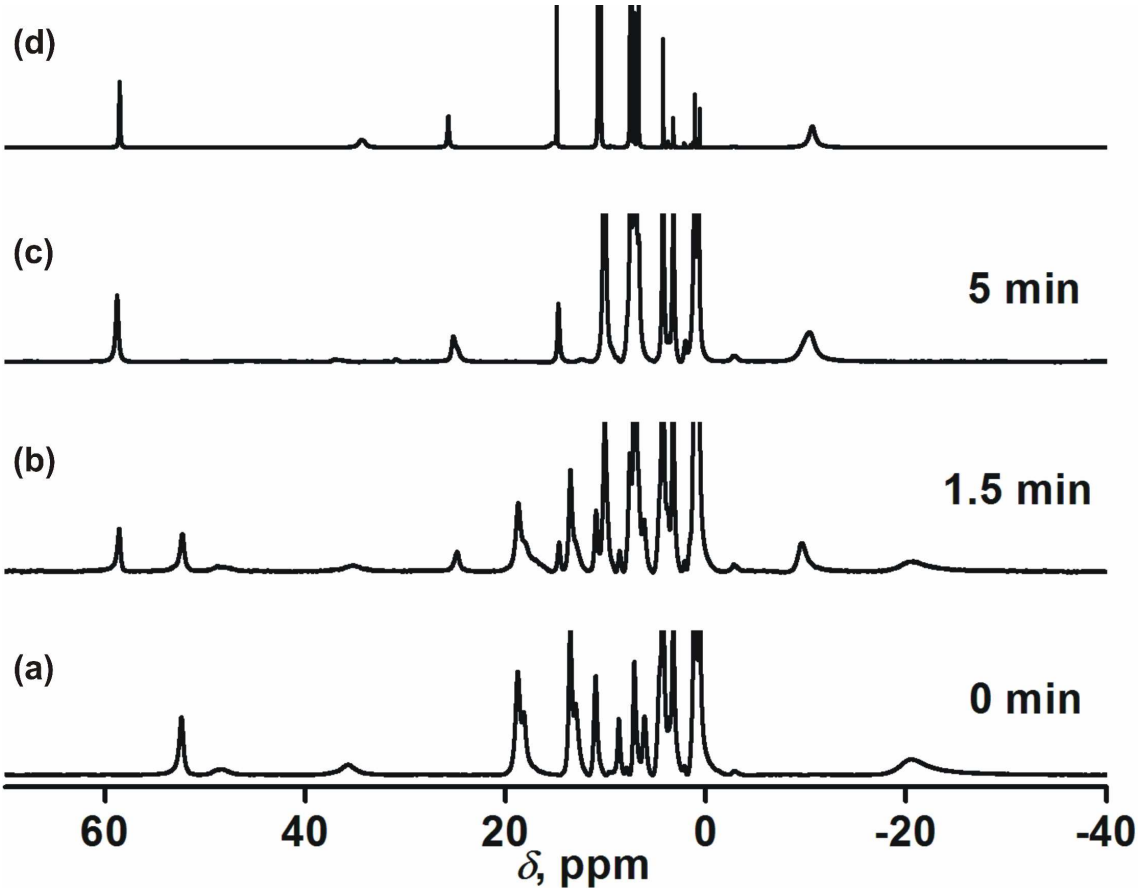

Figure S10 Time-dependent ^{1}H NMR (500 MHz, C_6D_6, 295 K) spectra during the reaction between [(Tp^{Ph2})Fe^{II}(PHAP)] (**1**) and O_2 (a-c). ^{1}H NMR spectrum of [(Tp^{Ph2})Fe^{II}(benzoate)] complex (d).

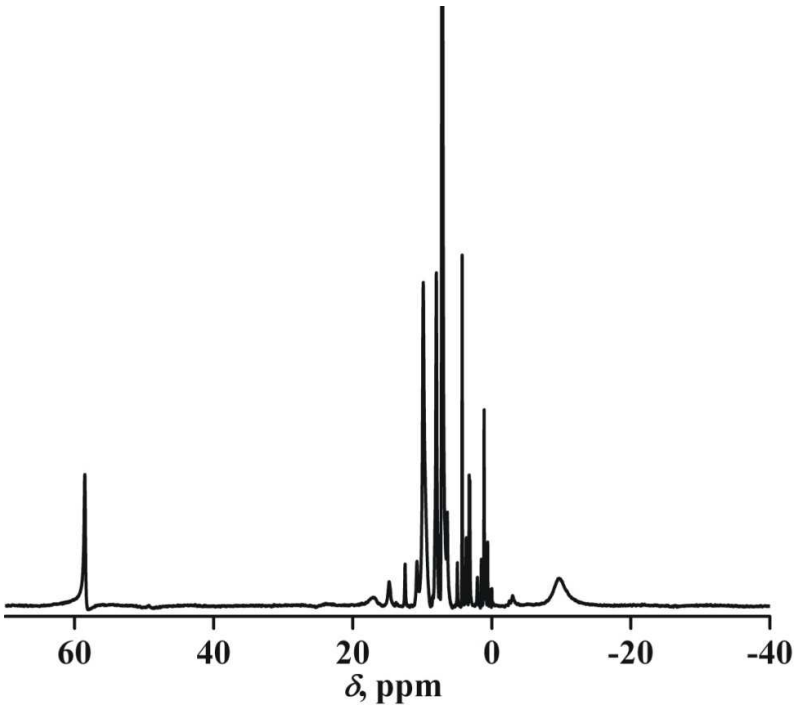

Figure S11 ^{1}H NMR spectrum (500 MHz, C_6D_6, 295 K) of the oxidized solution after the reaction of [(Tp^{Ph2})Fe^{II}(HCH)] (**2**) with O_2.

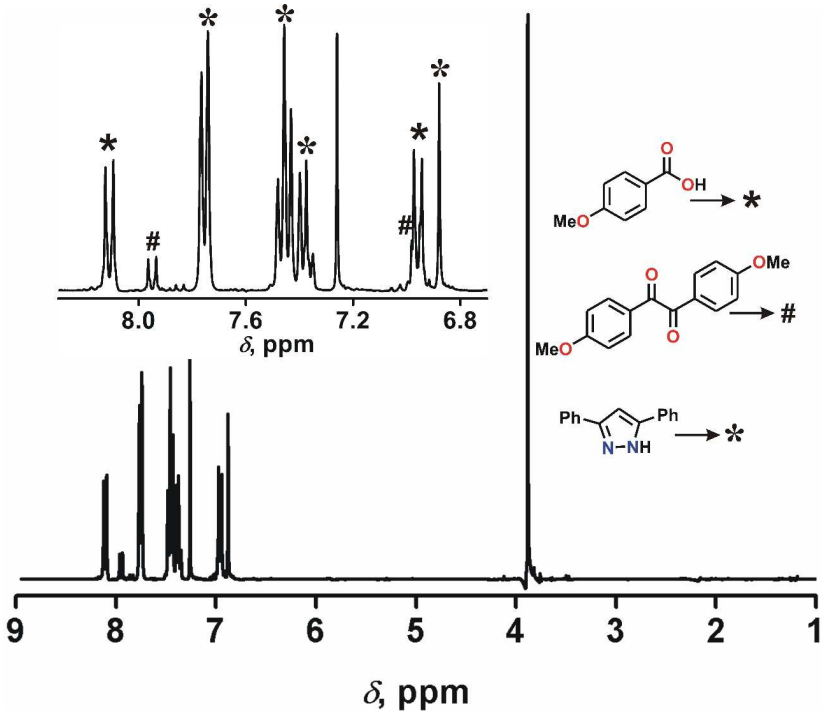

Figure S12 ^{1}H NMR (500 MHz, $CDCl_3$, 295 K) spectrum of organic products isolated from the oxidized solution of [(Tp^{Ph2})Fe^{II}(HBME)] (**3**).

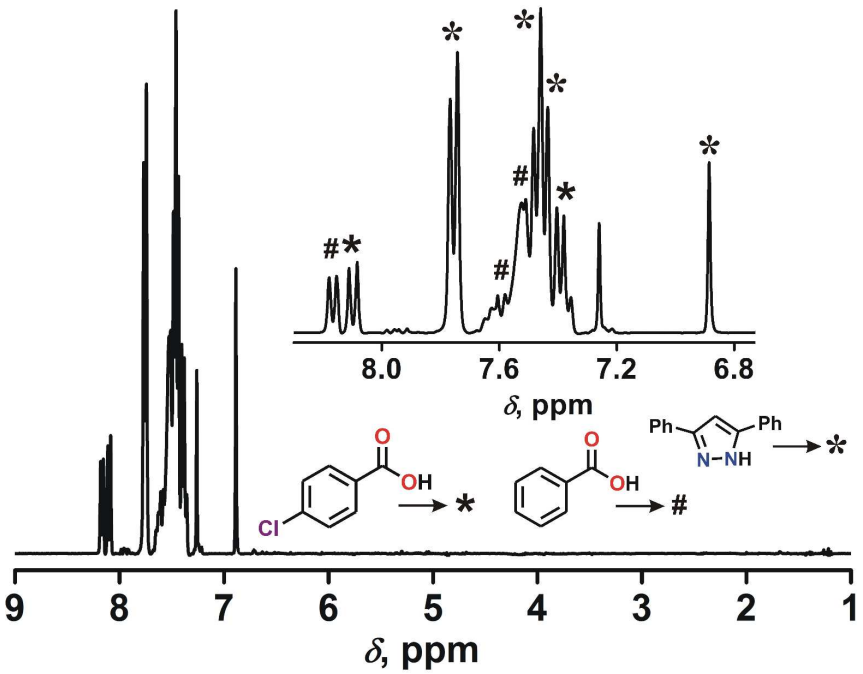

Figure S13 ^{1}H NMR (500 MHz, $CDCl_3$, 295 K) spectrum of organic products isolated from the oxidized solution of [(Tp^{Ph2})Fe^{II}(CHPE)] (**4**).

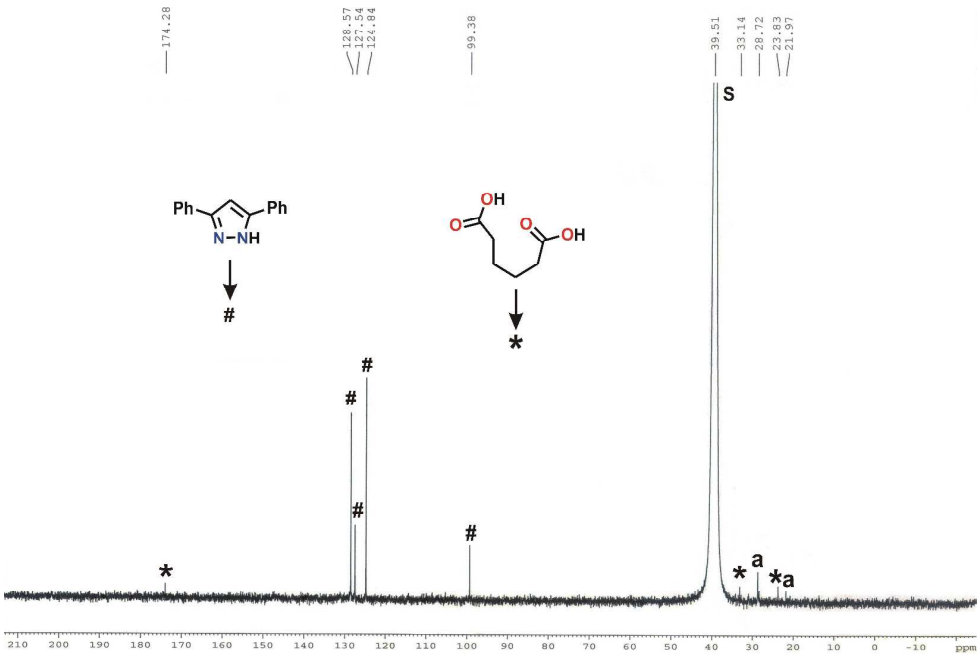

Figure S14 ^{13}C NMR (125 MHz, DMSO-d_6, 295 K) spectrum of organic products isolated from the reaction of [(Tp^{Ph2})Fe^{II}(HCH)] (**2**) with dioxygen. Peaks marked with 's' and 'a' are from residual solvents.

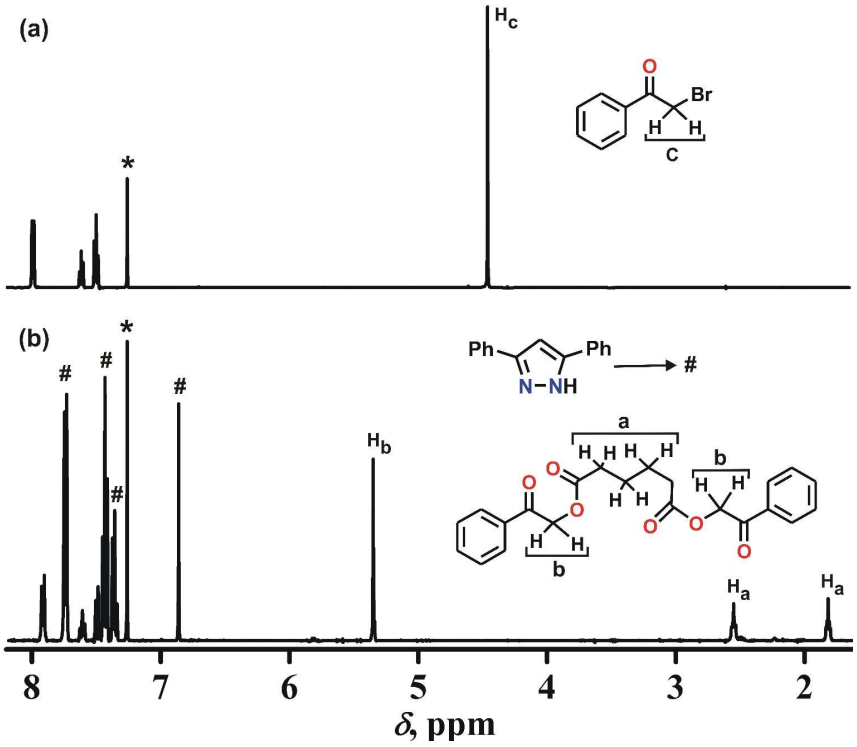

Figure S15 ^{1}H NMR (500 MHz, $CDCl_3$, 295 K) spectra of (a) α-bromoacetophenone and (b) esterified organic solution after the reaction of [(Tp^{Ph2})Fe^{II}(HCH)] (**2**) with dioxygen.

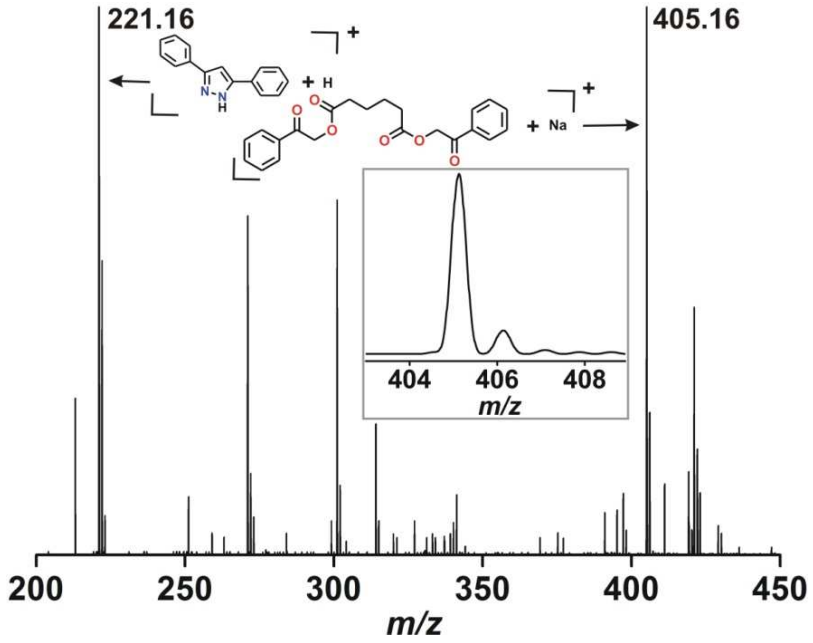

Figure S16 ESI-mass spectrum (positive ion mode in acetonitrile) of the phenacyl ester of adipic acid.

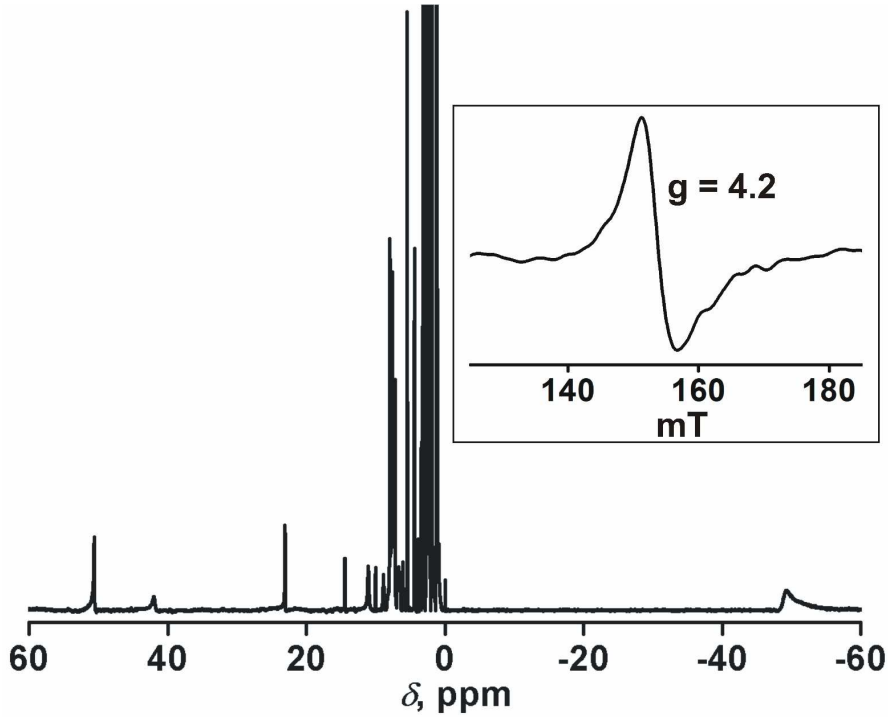

Figure S17 ^{1}H NMR spectrum (500 MHz, CD_3CN, 295 K) of the oxidized solution after the reaction of complex **5** with O_2. Inset: X-band EPR spectrum (at 77K) of the oxidized solution of **5**.

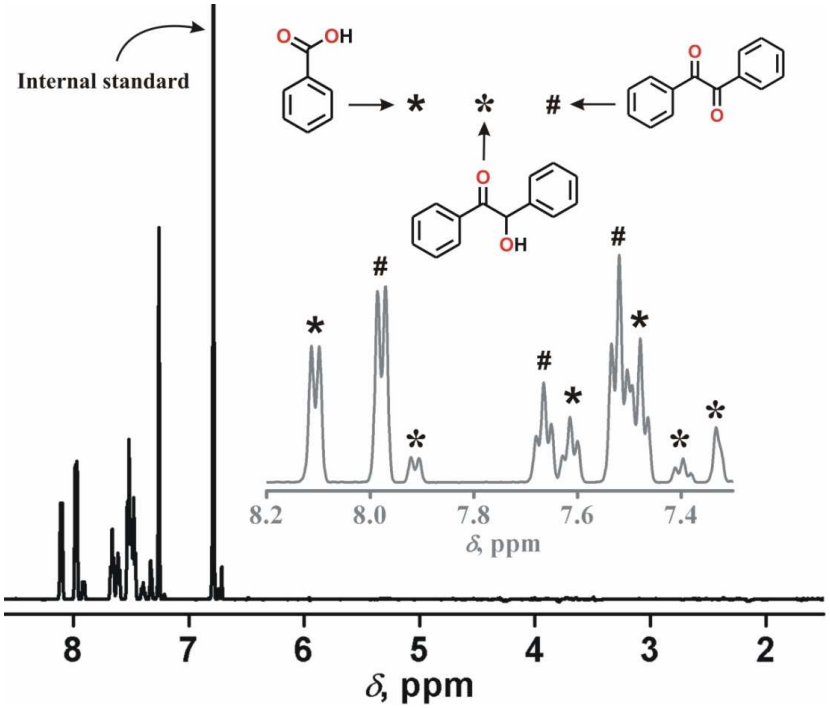

Figure S18 ^{1}H NMR (500 MHz, $CDCl_3$, 295 K) spectrum of the organic products derived from the oxidized solution of the perchlorate salt of **5**.

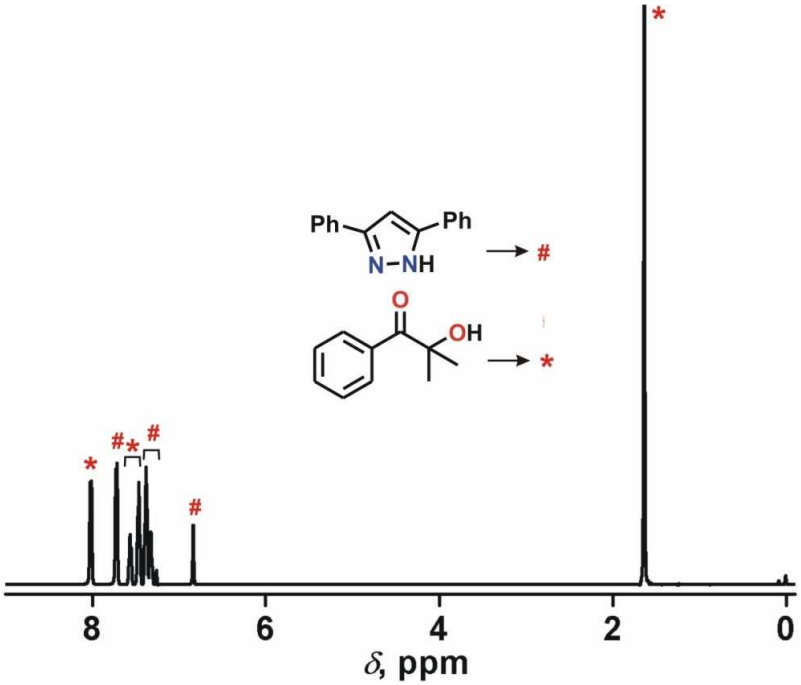

Figure S19 ^{1}H NMR (500 MHz, $CDCl_3$, 295 K) spectrum of organic products after the reaction of 2-hydroxy-2-methyl-1-phenylpropane-1-one with equimolar amounts of KTp^{Ph2}, iron(II) perchlorate and triethylamine in the presence of dioxygen.

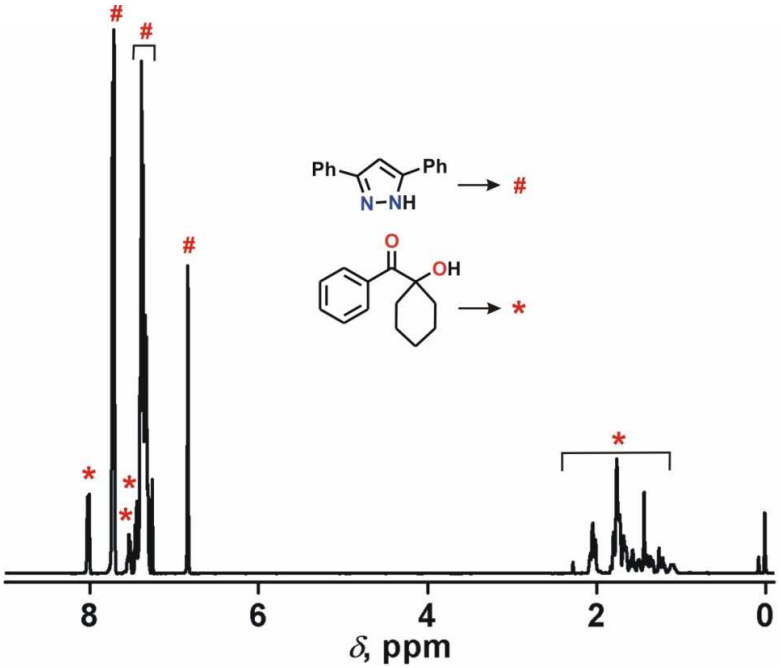

Figure S20 ^{1}H NMR (400 MHz, $CDCl_3$, 295 K) spectrum of organic products after reaction of 1-hydroxycyclohexyl-1-phenylmethanone with equimolar amounts of KTp^{Ph2}, iron(II) perchlorate and triethylamine in the presence of dioxygen.

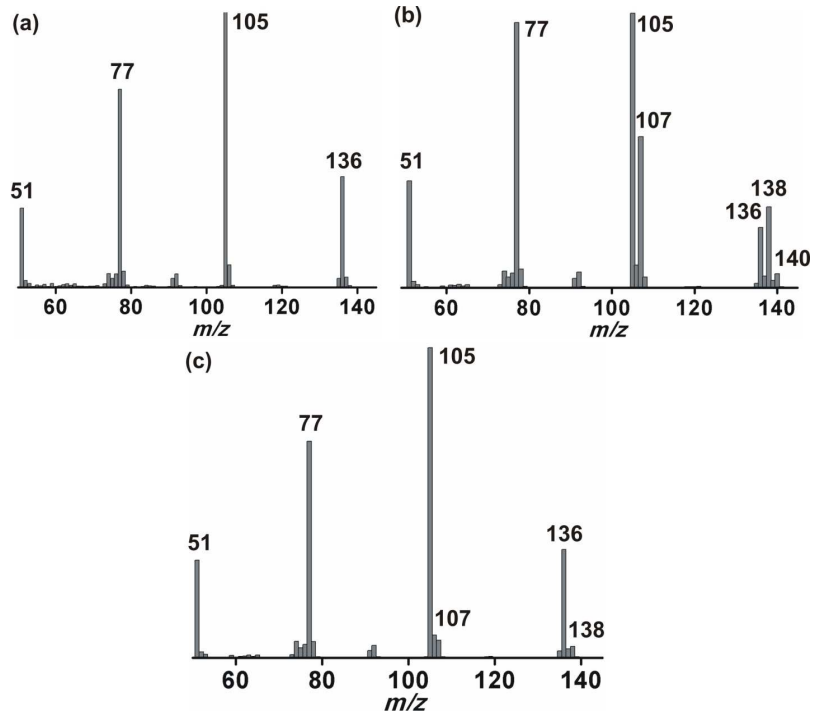

Figure S21 GC-mass spectrum of methyl benzoate derived from benzoic acid obtained from the oxidized solution of complex **1** after the reaction with (a) $^{16}O_2$, (b) $^{18}O_2$, and (c) $^{16}O_2$ and $H_2{}^{18}O$.

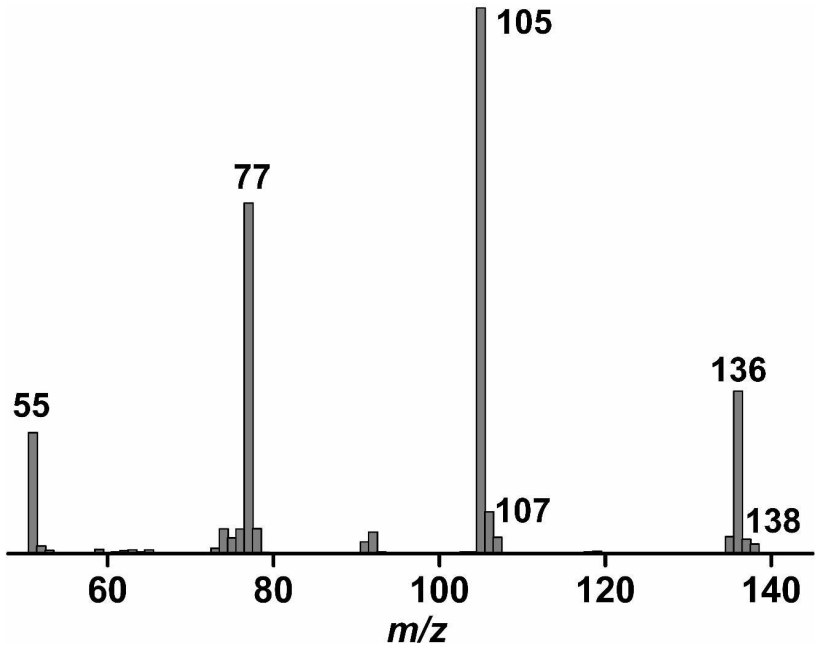

Figure S22 GC-mass spectrum of methyl benzoate derived from benzoic acid obtained from the oxidized solution of [(Tp^{Ph2})Fe^{II}(HAP)] (HAP = 2-hydroxyacetophenone) after the reaction with $^{16}O_2$ and $H_2{}^{18}O$.

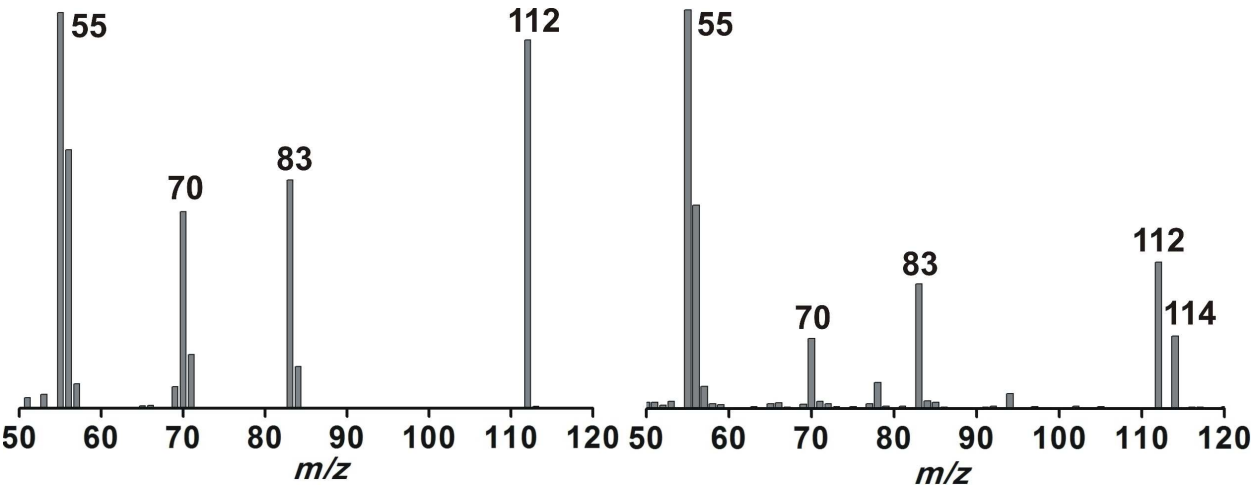

Figure S23 GC-mass spectrum of cyclohexane-1,2-dione isolated from the reaction of complex **2** with (a) $^{16}O_2$ and (b) $^{16}O_2$ and $H_2{}^{18}O$.

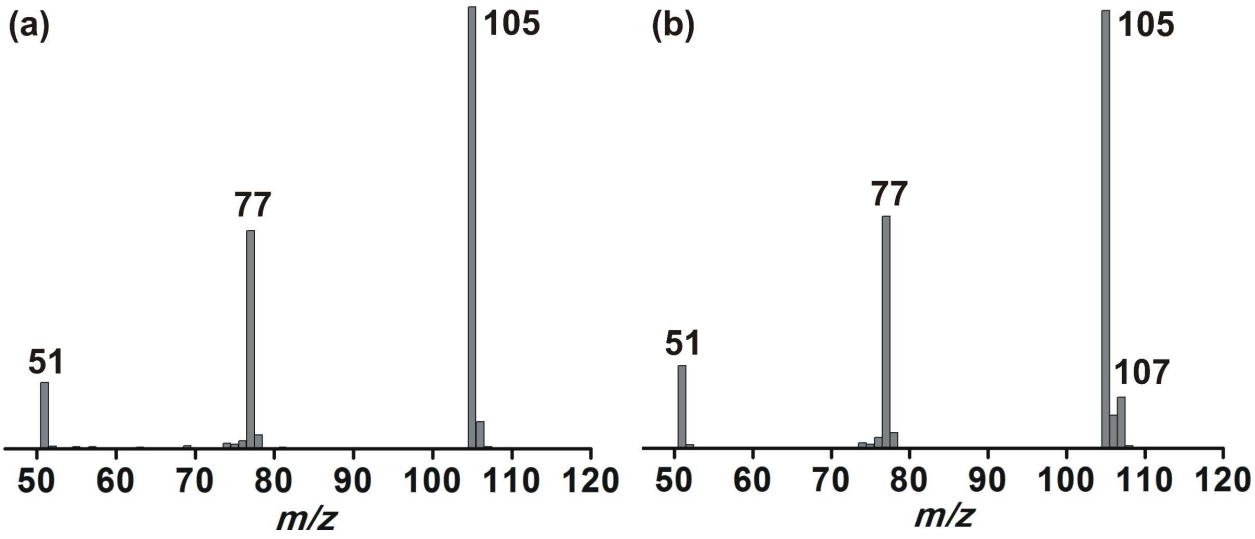

Figure S24 GC-mass spectrum of benzil derived from the oxidized solution of **5** after the reaction with (a) $^{16}O_2$ and with (b) $^{16}O_2$ in the presence of $H_2{}^{18}O$.

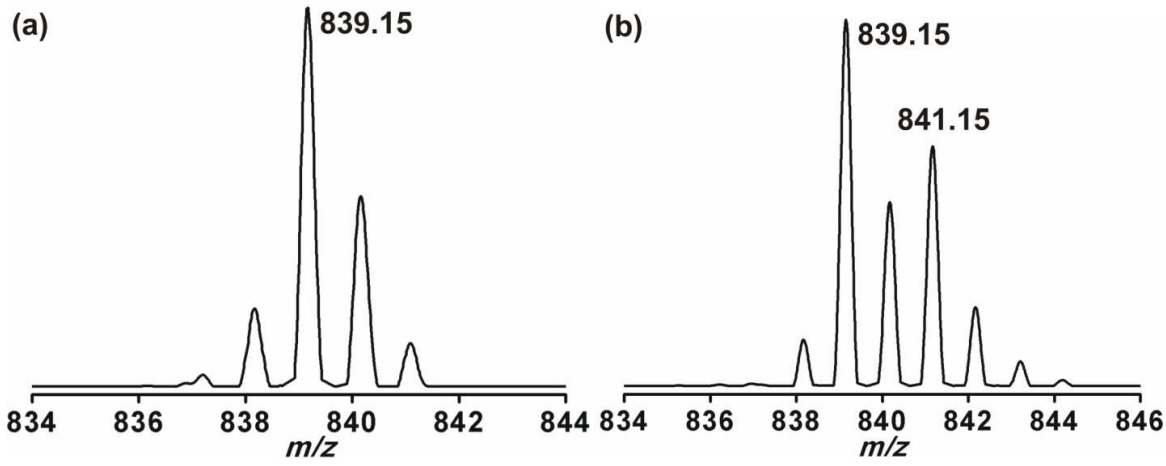

Figure S25 ESI-mass spectrum (positive ion mode in acetonitrile) of (a) **2** and (b) **2** + $H_2{}^{18}O$ under inert atmosphere.

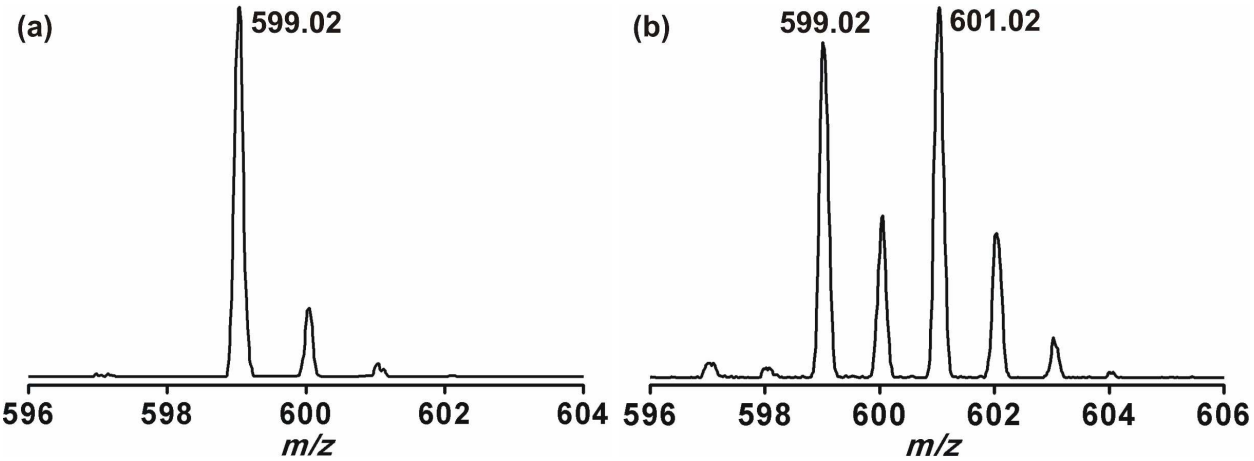

Figure S26 ESI-mass spectrum (positive ion mode in acetonitrile) of (a) **5** and (b) **5** + $H_2{}^{18}O$ under inert atmosphere.

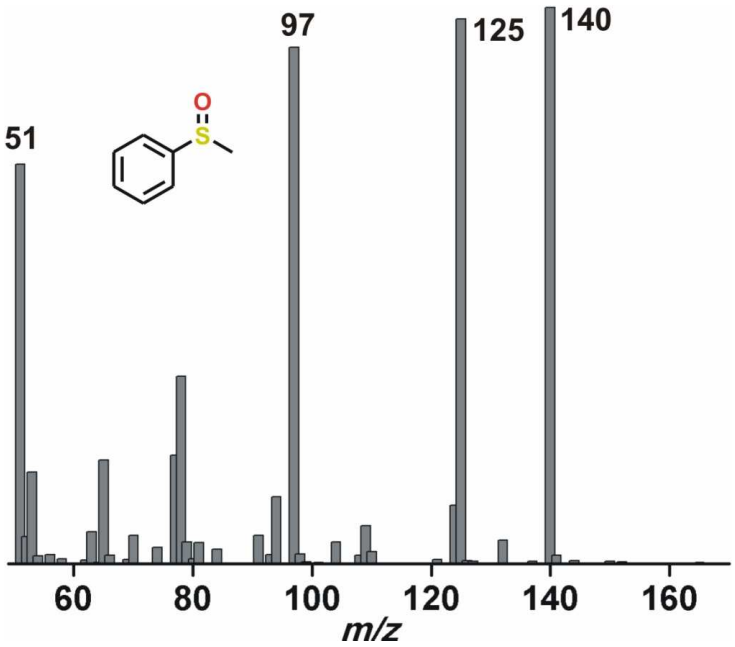

Figure S27 GC-mass spectrum of thioanisole oxide formed in the reaction of **1** with thioanisole (10 equiv) and dioxygen.

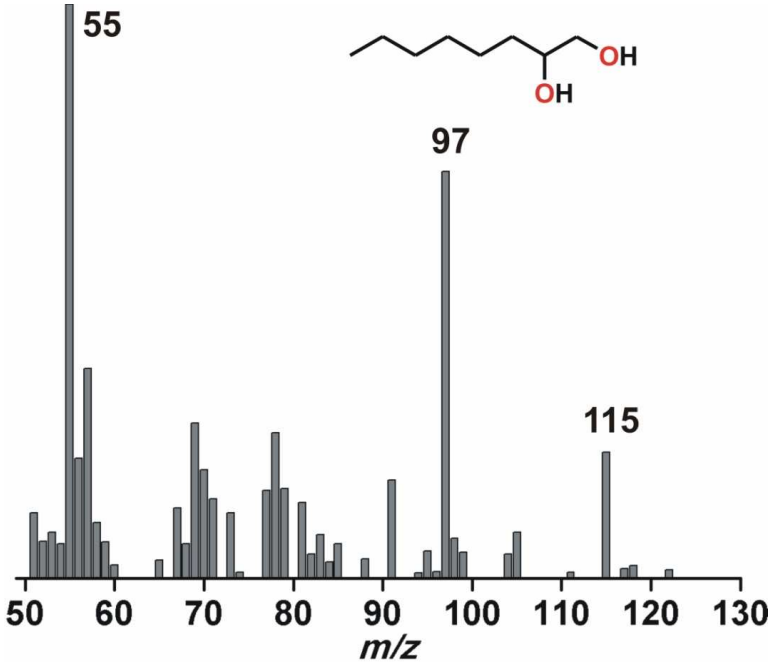

Figure S28 GC-mass spectrum of octane-1,2-diol formed in the reaction of **4** with 1-octene (100 equiv) and dioxygen.

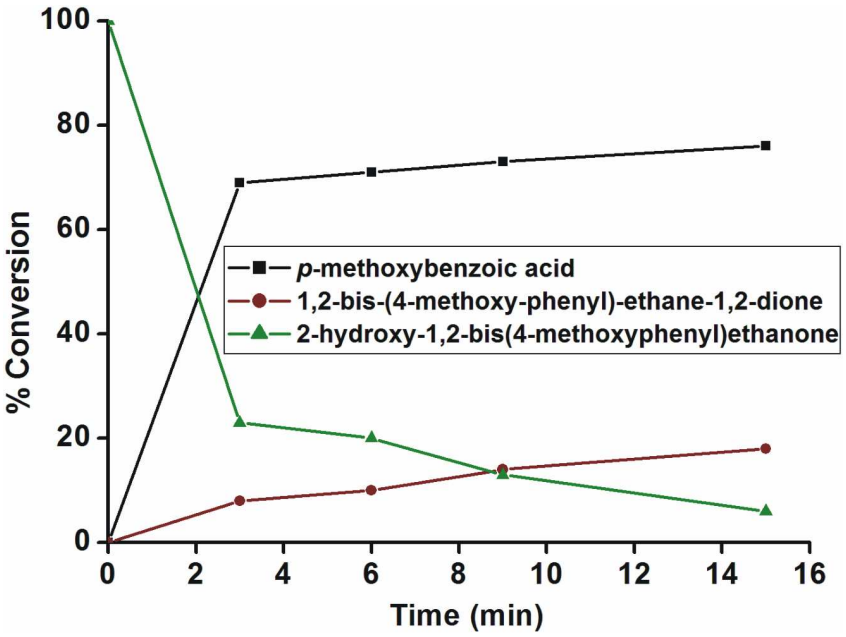

Figure S29 Time-dependent formation of products in the reaction of complex **3** with dioxygen.

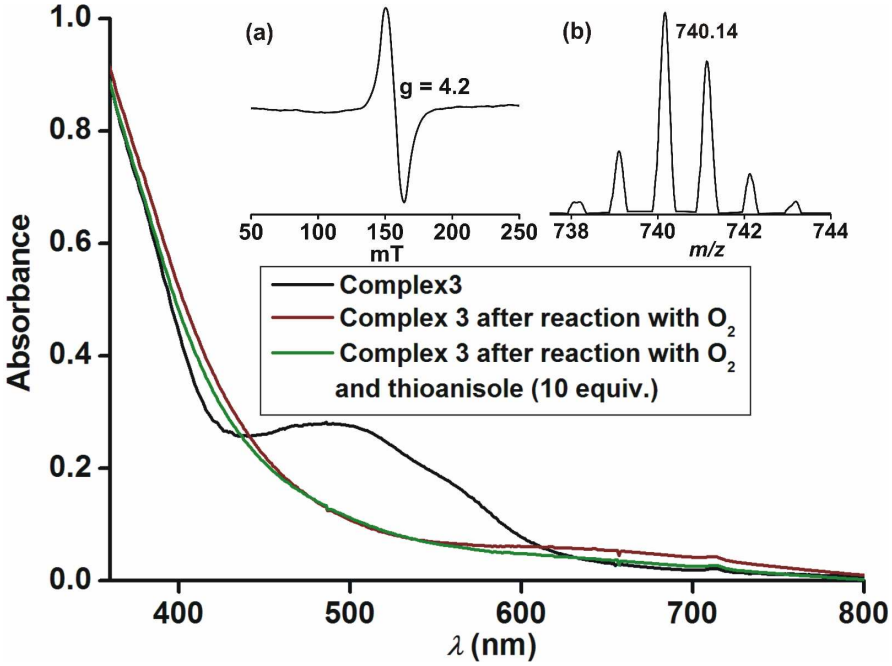

Figure S30 Optical spectra of **3**, after the reaction of **3** with dioxygen, and after the reaction of **3** with dioxygen in the presence of thioanisole (10 equiv). Inset: (a) X-band EPR (at 77K) spectrum, and (b) ESI-MS (positive ion mode) of the final oxidized solution of **3**.

Table S1 ESI-MS (positive ion mode) peak assignments of the iron(II)-α-hydroxy ketone complexes.

Complex	Ion peaks (*m/z*)	Peak assignment
1	725.12	$[(Tp^{Ph2})Fe]^+$
	743.15	$[(Tp^{Ph2})Fe(H_2O)]^+$
	766.22	$[(Tp^{Ph2})Fe(CH_3CN)]^+$
2	725.12	$[(Tp^{Ph2})Fe]^+$
	766.22	$[(Tp^{Ph2})Fe(CH_3CN)]^+$
	839.10	$[(Tp^{Ph2})Fe(HCH) + H]^+$
	945.10	$[(Tp^{Ph2})Fe(3,5\text{-diphenylpyrazole})]^+$
3	725.23	$[(Tp^{Ph2})Fe]^+$
	766.29	$[(Tp^{Ph2})Fe(CH_3CN)]^+$
	945.24	$[(Tp^{Ph2})Fe(3,5\text{-diphenylpyrazole})]^+$
4	725.13	$[(Tp^{Ph2})Fe]^+$
	945.14	$[(Tp^{Ph2})Fe(3,5\text{-diphenylpyrazole})]^+$
	971.21	$[(Tp^{Ph2})Fe(CHPE) + H]^+$
5	333.09	$[(6\text{-}Me_3\text{-TPA}) + H]^+$
	599.09	$[(6\text{-}Me_3\text{-TPA})Fe(PHAP)]^+$
6	333.23	$[(6\text{-}Me_3\text{-TPA}) + H]^+$

……